



A mini-review: How reliable is the drop casting technique?

Archana Kaliyaraj Selva Kumar¹, Yifei Zhang¹, Danlei Li, Richard G. Compton^{*}

Physical and Theoretical Chemistry Laboratory, Department of Chemistry, University of Oxford, South Parks Road, Oxford OX1 3QZ, United Kingdom

ARTICLE INFO

Keywords:

Particle modified electrodes
Nanoparticles
Electro-catalysts
Coffee ring effect

ABSTRACT

The simple, easy and rapid technique of “drop casting” is widely used to prepare the surface of chemically modified electrodes in which the modifying layer is composed of particles such as nanotubes or nanoparticles and used for electro-catalysis notably for chemical sensing as well as materials evaluation. However, meaningful voltammetry requires the formation of uniformly modified surfaces for which the coffee ring and its related effects, which are overviewed, present a significant limitation on the reproducibility of the drop casted surfaces. Approaches for amelioration of the coffee ring effect by various methods are discussed.

1. Introduction

The search for improved electrochemical sensors of the amperometric variety has stimulated the study of an astonishing diversity of modified electrodes in the quest for enhanced sensitivity and selectivity [1–8]. One approach has become ubiquitous over the last two decades and involves the modification of the surfaces of macro-electrodes with a layer of particles. The substrates are often made of carbon in some forms, such as glassy carbon or graphite [9–14] for reasons of ready availability and, often, low cost although doped diamond [15–17] and single-crystal [18–20] forms are also used. The modifying layer is selected with the hope or anticipation of useful enhancement of the electrochemical response towards some desired target analyte. Thus the particles might for example act as electro-catalysts in the case they are electrically conductive, or, for the case of electrically insulating particles, via the adsorptive pre-concentration of the target prior to analysis on the underlying substrate electrode [21]. The interpretation of the observed voltammetry at a fundamental level is complicated [22–25], although in practice often an ‘analytical response’ is simply sought and it is the case that without any doubt the fabrication, assessment and application of particle modified electrodes (PMEs) is a widespread phenomenon, apparently unlimited by the availability of novel, chemically diverse materials for evaluation!

Whilst the extent to which such PME can realistically markedly enhance the sensitivity of amperometric analytical detection has been questioned [21,26], this paper addresses a different concern now from

an experimental perspective. In particular we note that the overwhelmingly popular approach for the preparation of PME is via the method of drop casting (see Fig. 1). In this method, a drop of liquid containing a suspension of the particles of interest is first deposited (literally ‘drop casted’) on the surface of the electrode to be modified, ideally exclusively confined to the conductive electrode without, for example, over-spillage onto the insulating surround.

If the particles are to act via an electro-catalytic mechanism then a surprisingly small number of particles need to disperse over the electrode surface to ensure a diffusional response that, in terms of which potential the electrode process takes place, is characteristic of the particles and not that of the underlying substrate electrode. In other words, that the catalytic signal is observed at lower potentials than would be seen on the substrate and is such that all the material diffusing to the electrode surface is consumed at the particles before a voltammetric sweep reaches the potential required for reaction on the underlying electrode. This requires strong overlap of the diffusion fields associated with the electro-catalyst particles such that the coverage of the latter leads to overall linear diffusion to the electrode [27–31] as illustrated in Fig. 2 for different scan rates; Fig. 2d shows the limit of full diffusional overlap.

Specifically, theory shows that for measurements of solution phase species on a timescale, t , that for strong overlap the particles need to be within a distance of $\delta = (6Dt)^{1/2}$ of one another where D is the analyte diffusion coefficient [32]. This length corresponds to the root mean square distance diffused (in 3-dimensions) in the time t . Then the PME

^{*} Corresponding author.

E-mail address: Richard.compton@chem.ox.ac.uk (R.G. Compton).

¹ These authors contributed equally to this work.

signal is dominated by the particles, not the substrate. Typically for a species with a diffusion coefficient of $10^{-5} \text{ cm}^2 \text{ s}^{-1}$ for a voltammetric timescale² of a few seconds the size of δ can be as large as of the order of ca 100 μm . Hence for a random array of fully dispersed particles a coverage of say just 10^5 particles per cm^2 may thus suffice. In analytical practice, however, much larger amounts are deposited partly because in the case of sparse coverages it cannot be guaranteed that all particles are in electrical contact with the substrate or are not aggregated [33–35]. In the case of PME's which function via adsorptive pre-concentration then thick layers are essential to provide some enhancements of signal although the conflicting demands of both a large strong adsorption and the rapid release of the accumulated analyte for electrochemical detection are not always appreciated [21].

From an experimental perspective, regardless of whether sub-monolayer or thick layers of particles are desired, it is important to know if the extent to which the electrode has been homogeneously modified (or not) when using the drop casting approach for fabrication. For potentials at which catalysis takes place on the particles, the modified electrode will only exhibit linear diffusion to its geometric area in the absence of macroscopic patches of naked unmodified electrode. Here the size of the patches that must be avoided implies a larger size compared to the diffusion distance δ introduced above via the Einstein equation [32].

The purpose of this review is to explore to what extent drop casting can result in reproducible surfaces and the extent to which heterogeneity is induced [36]. In particular, we describe and then consider the physical basis for the so-called coffee ring effect and related issues as well as approaches for their mitigation.

2. Origin of the coffee ring effect

The evaporation of sessile droplets containing suspended particles

under ambient conditions often forms a ring-like pattern which is macroscopic in size and visible by eye upon drying. This phenomenon was notably observed, highlighted and interpreted by Deegan et al. [37], in respect of coffee stains, where the periphery of the ring was seen to be concentrated with the non-volatile solute particles in contrast to the centre of the stain: this phenomenon has been labelled as the “coffee ring effect” (CRE).

The physical requirements to observe a ring pattern originate in the ‘pinning’ of the contact line at the edge of the droplet by surface tension forces. Contact line pinning restricts any further spreading of the solvent and a radial outward capillary flow of the solvent from the centre is observed towards the contact line, driven by evaporation since the evaporation is greatest at the edge which is more ‘ventilated’ than the centre of the drop [38]. This is due to a larger free space at the edge of the droplet which induces the evaporation of more solvent molecules than in the centre. Since the evaporation flux at the periphery is comparatively more than at the centre of the droplet this leads to greater solvent loss at the contact line. The loss is compensated by a flow of solvent from the centre along with the non-volatile solute particles. The rate of local evaporation is, therefore, a major factor controlling the radial outward flow of the solution. The magnitude of the evaporation flux depends on the radius, r , of the droplet, height, h , of the droplet above the centre and the contact angle Θ_r with the velocity of the particles reflecting the spatial heterogeneity of the evaporative flux (see Fig. 3). The coffee ring effect is noted for its malign consequences related to the disruption of otherwise uniform distribution of particles for example importantly in ink-jet printing [39–41], functional coating with ordered structures functional nanomaterials and in electronics [42–44].

As noted above the consequence of the coffee ring effect is that the particles tend to form ring-like patterns on the surface. Typical observations are shown in Fig. 4, where Anyfantakis et al. studied negatively charged PS particles coated with acrylic acid (AA) [45]. One drop of a PS

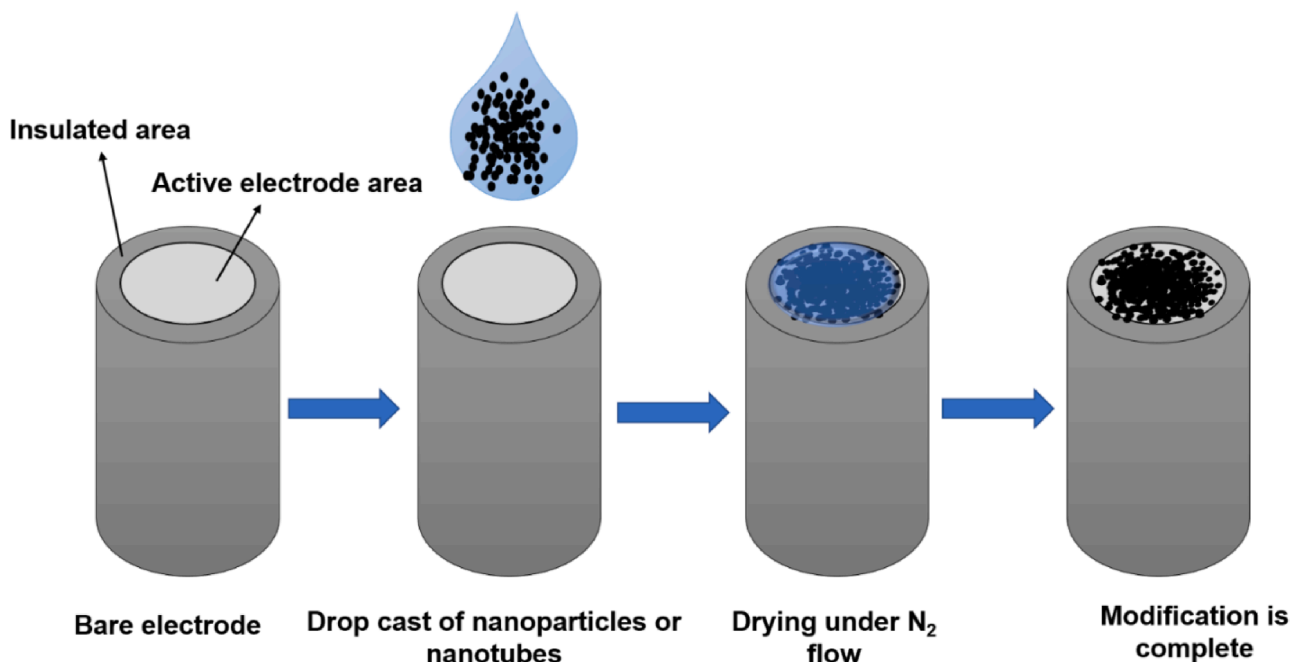


Fig. 1. A schematic showing the drop casting of nanoparticles or nanotubes onto an electrode.

² The “voltammetric timescale” is the time of a voltammetric sweep encompassing the peak leading to the electrode reaction of interest. The timescale of the sweep is of an order of magnitude of (RT/vF) where v is the voltage scan rate.

particle suspension was casted onto the substrate and dried over 300 s (Fig. 4 a, b and c). During the evaporation of a 0.5 μL of droplet with PS-AA particles, weak aggregation at the liquid–gas (LG) interface was observed (Fig. 4a and 4d) [45]. The image taken at 245 s, showed that the PS-AA particles became packed at the edge of the droplet when most of the solvent had evaporated (Fig. 4e) and the ring-like pattern could be

observed clearly (Fig. 4b) on complete evaporation. This again shows that along with the solvent evaporation at the droplet edge, there is a flow of solvent with the particles from the centre towards the edge. The dry deposit was thus a classic coffee ring pattern (Fig. 4c and 4f).

In another insightful study, Park and Moon [39] used silica microspheres dispersed in water-based ink and a coffee ring was formed after evaporation of the droplet (Fig. 4h). SEM images of both the edge (Fig. 4g mid) and the centre (Fig. 4g bottom) were recorded. Most of the microspheres became agglomerated and stacked at the edge due to the evaporatively driven capillary flow (Fig. 4g middle). At the same time there were much fewer particles at the centre of the dried droplet (Fig. 4g bottom).

The surface hydrophobicity/hydrophilicity can influence the formation of the ring pattern. In the cases of hydrophilic substrates such as silica glass or polycarbonates, the contact line can move towards the centre of the droplet forming not a ring-like pattern but instead a concentrated stain of the non-volatile solute particles at the centre. Such an effect was shown experimentally by Y. Feng Li et al., with 9.25 μL CuSO_4 aqueous solution (blue coloured) drop casted on a smooth silica glass. Often, in contrast, when a rough substrate like graphite is used, the contact line gets firmly pinned and the solute particles become adsorbed on the substrate without the movement of the contact line and thus forms a coffee ring like pattern depositing the particles at the edge of the

contact line [46].

3. Approaches to the amelioration of the coffee ring effect

The distribution of non-volatile solute particles on the substrate is governed by various factors as discussed above. Many approaches have been taken with the aim of suppressing the coffee ring effect to obtain a more uniform distribution of solute particles. Most of these methods are aimed in altering or affecting the capillary flow, and/or unpinning the contact line and preventing the transport of solute particles to the edge of the droplet. The following are some methods which have proven effective in reducing the coffee ring effect in specific cases.

3.1. Super hydrophobic surfaces

Super hydrophobic surfaces can help in the suppression of the CRE. One mechanism is by reducing the effectiveness of the contact line pinning by making it slip over the hydrophobized surfaces. The slipping of the contact line pinning induces an inward circulatory flow of the solute particles forming a more homogeneous deposition. Both chemical and physical modifications are involved in making a surface super-hydrophobic but can be prohibitively expensive for routine uses [47–51] as well as changing the chemical nature of the surface, which

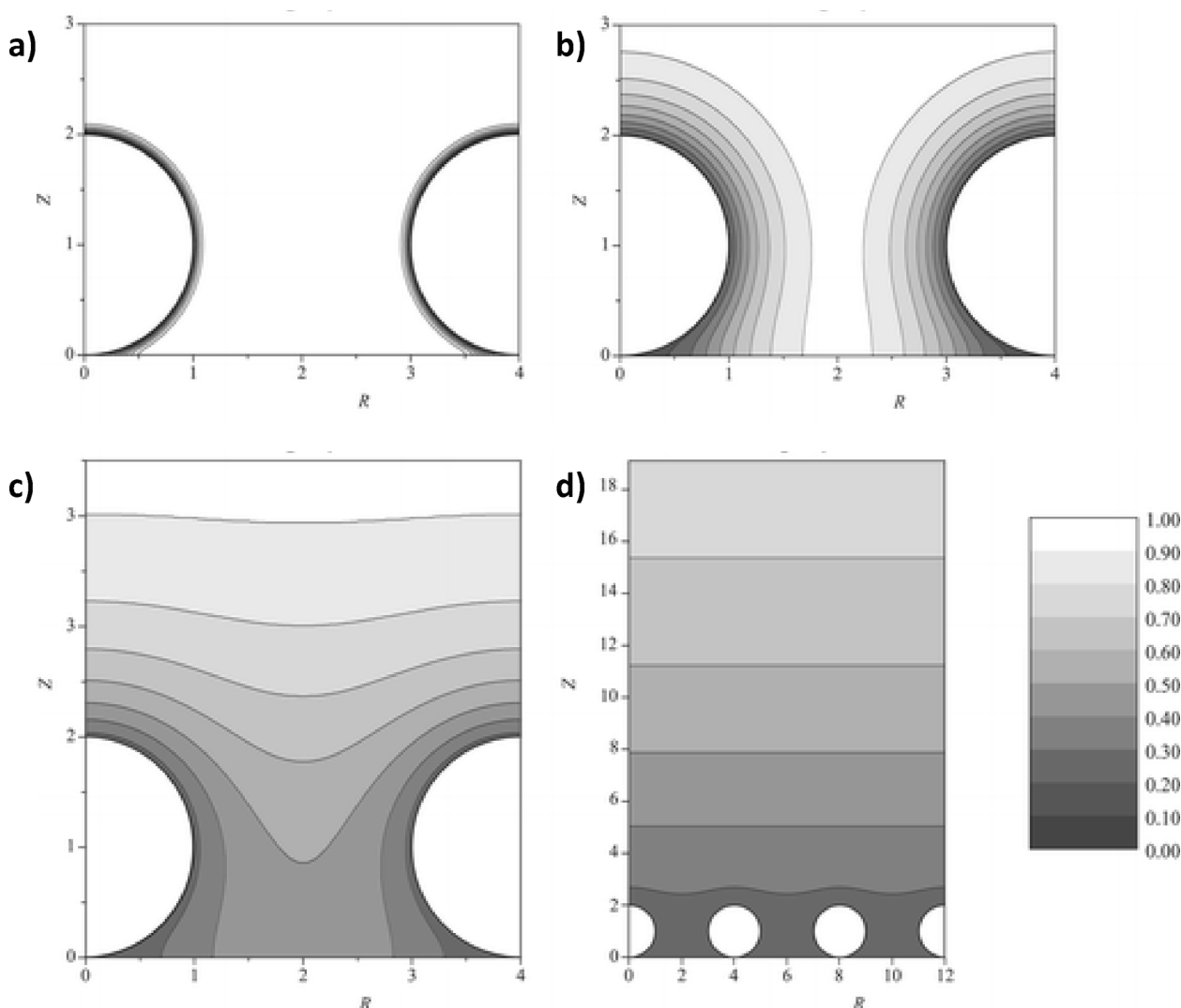


Fig. 2. Simulated concentration profiles at an electrode modified with spherical particles for the relative inter-particle spacing shown and for four different scan rates of decreasing magnitude from a) to d). The concentration profiles are those at the linear sweep peak potential. Full diffusional overlap is only attained in d).

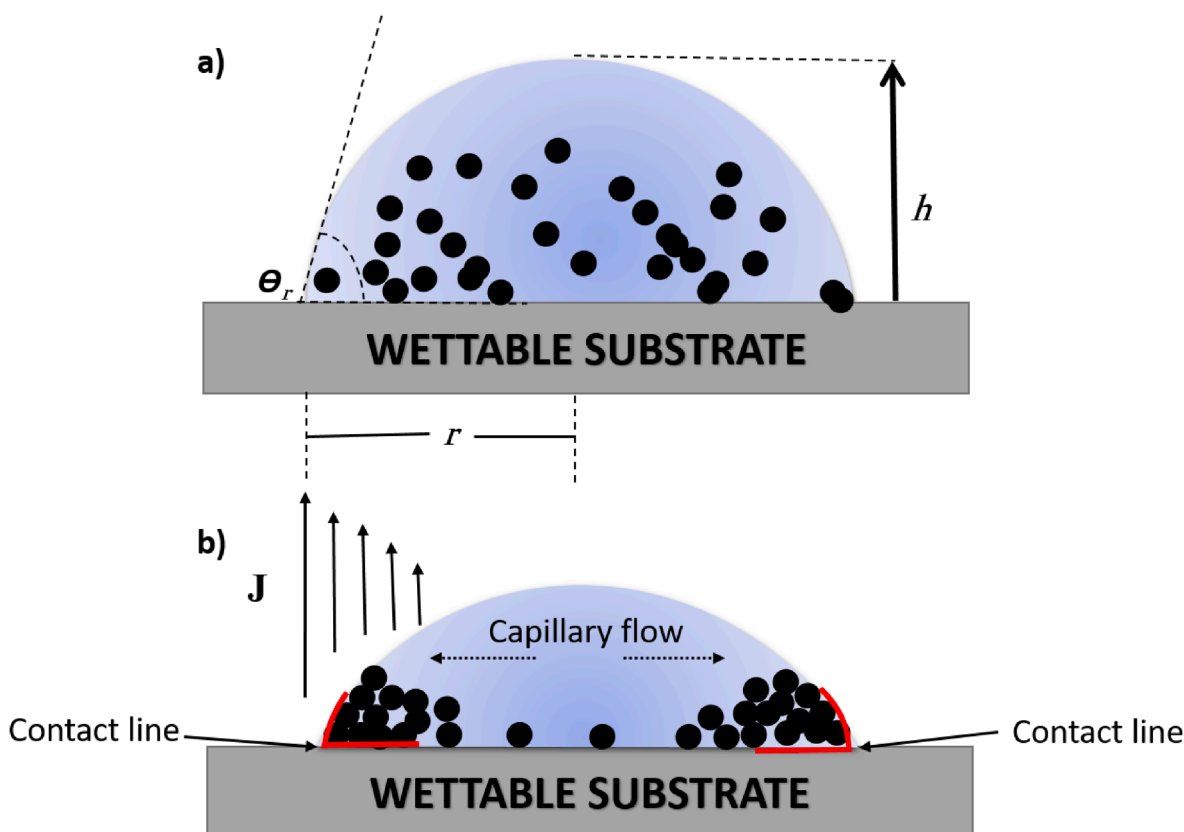


Fig. 3. A scheme showing a) a droplet containing particles on a solid substrate and b) capillary flow from centre to the edge keeping the contact line fixed during evaporation. Particles in the droplet are moved to the edge due to the capillary flow. h = height of droplet; Θ_r = contact angle; r = radius of the droplet; J = evaporation flux.

may be important if the latter is to be an electrode.

In a study by Moon et al., octadecyltrichlorosilane (OTS) was applied onto a silica substrate to create a hydrophobic surface [47]. The OTS-modified self-assembled monolayers (SAMs) produced a Wenzel (Fig. 5a) or Cassie (Fig. 5b) state. Thus, when a single ink droplet was evaporated on the substrate, a circulatory fluid flow was generated, which was opposite to the capillary flow, and reduced the coffee ring effect by transporting particles back to the centre. Similarly Jiang et al., deposited oil ink onto a TiO_2 substrate [50], forming a super-hydrophobic surface. When a latex droplet was evaporated on the surface, the inward circulatory flow again counteracted the outward capillary flow, pressed and a homogeneous surface was produced. These two examples very clearly demonstrate that chemically modified hydrophobic surfaces can reduce the coffee ring effect but are probably not suitable for general electrochemical applications.

Meanwhile, some physical (as opposed to chemical) modification methods have also been applied to create a super hydrophobic surface. Snoeijer's and Yang's group used silicon pillar arrays to avoid the coffee ring effect [48,49]. The array increased the roughness of the surface creating either Wenzel or Cassie states for supported droplets. When a colloid-containing droplet was evaporating on the microarrays, the contact line was unpinning due to the low surface tension and the particles aggregated in the centre by circulatory flows.

In general, the coffee ring effect is either reduced or suppressed on super hydrophobic surfaces. The method of electro-wetting again involves de-pinning of the contact line. Although, super hydrophobic surfaces prevent the pinning of the contact line by slipping, at higher concentrations, the solute particles often stick firmly to hydrophobic substrates [52,53].

3.2. Electrowetting

In such cases, electro-wetting may succeed wherein the sessile droplet is deposited on an electrode and a voltage is applied between the droplet and the electrode. This overcomes the pinning forces at the contact line, making it more mobile and not static [53–55]. Eral et al., studied how to tune the contact line and contact angle by changing the voltage used [52]. Drops of an aqueous polystyrene suspension containing 10 mM LiCl were deposited onto glass substrates with conductive indium-tin-oxide (ITO) layers covered with an insulating 5 μm thick layer of SU8 resist. The latter is an epoxy-based negative photoresist which becomes cross-linked due to exposure to UV. The drops were electrically grounded via immersing a 50 μm diameter Pt wire near the bottom of the drop. AC voltages (200 V_{rms}) with variable frequencies of 6 Hz – 100 kHz were applied to the ITO layer. A scheme of the setup is shown in Fig. 6a. ring-like pattern could be observed clearly without electro-wetting (Fig. 6b) but the resulting deposit shrank in size when the AC current was applied (Fig. 6c and 6d). However, if the frequency reached 100 kHz, the pattern after evaporation became as shown in Fig. 6e, showing that the electro-wetting could usefully reduce and suppress the coffee ring effect.

3.3. Anisotropic particles

The shape of the non-volatile solute particles can influence the CRE, due to particle–particle interactions while drying. These can be either relatively long - or short - ranged depending on the shape and size of the particles. P J Yunker et al., experimentally studied the suppression of the CRE by modifying the shape of the solute particles from spherical to ellipsoidal; spherical polystyrene particles (diameter = 1.3 μm) when treated with polyvinyl alcohol became stretched into ellipsoids [56].

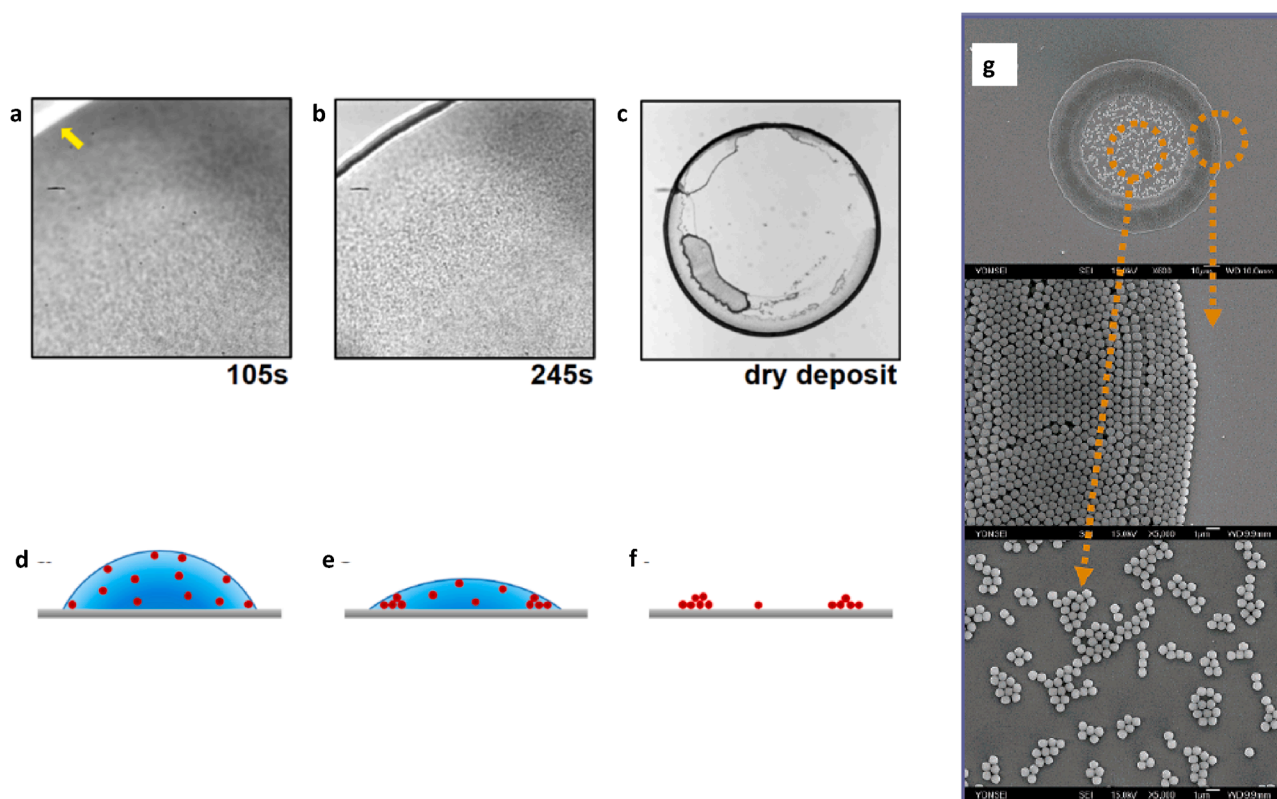


Fig. 4. a) – c) Snapshots of a droplet containing a suspension of PS-AA (see text) particles during evaporation and imaged at 105 s (a), 245 s (b), and after full drying deposit (c). The scale bars are 500 μm for the high- (a and b) and low-magnification (c) images. d) – f) cartoons of the PS-AA droplet during evaporation at 105 s (d), 245 s (e), and dry deposit (f). Reprinted with permission from Anyfantakis et al. *Langmuir*, 2015; 31(14):4113–20. Copyright (2015) American Chemical Society. Ref. [45]. g) SEM images of deposit patterns composed of the silica microspheres produced by ink-jet printing a single ink-jet droplet of water-based ink. The ink concentration was 4 vol% and the substrate was a hydrophilic Si wafer. Reprinted with permission from Park and Moon. *Langmuir*, 2006; 22(8):3506–13. Copyright (2006) American Chemical Society. Ref. [39].

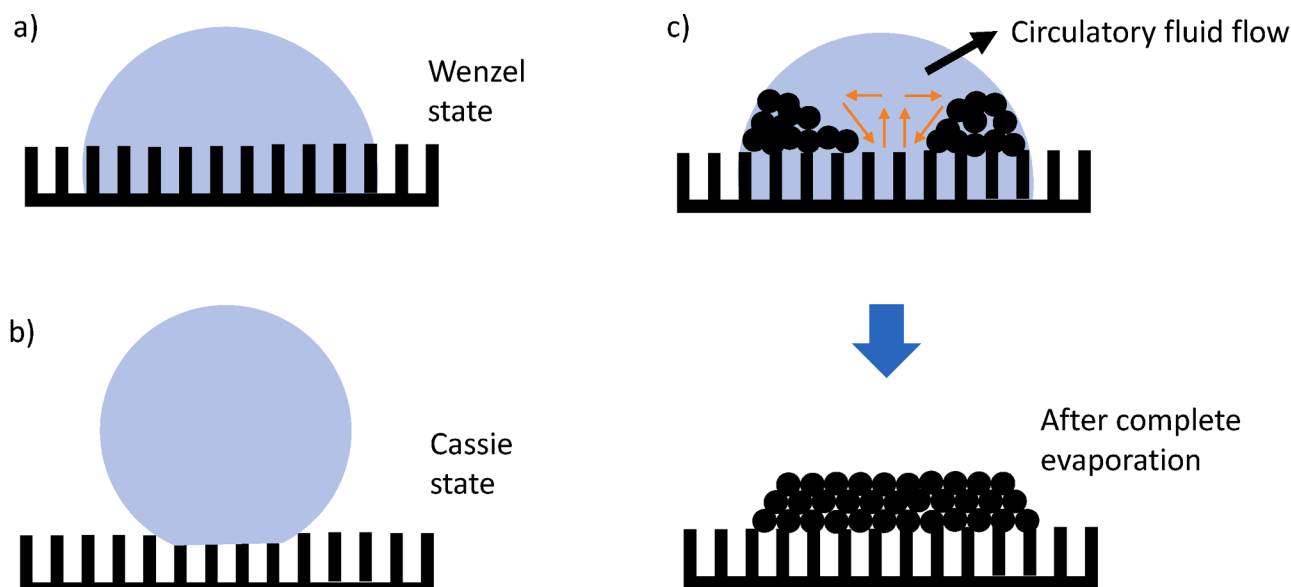


Fig. 5. A schematic diagram showing a) a Wenzel state, and b) a Cassie state of a hydrophobic surface, and c) the circulatory fluid flow that reduces the coffee ring effect so generating a more uniform distribution of particles after evaporation.

These ellipsoidal particles exhibited stronger long ranged inter-particle capillary attractions between the solute particles. The resulting interaction of particles during evaporation caused formation of clumps of the solute particles and restricted the outward flow of the solute particles

towards the contact line. The pattern of the drop casted film was shown to reflect the major and minor axis ratio α which for spheres is 1, and deviates from 1 for deformed shapes like ellipsoids. Fig. 7 shows the schematic representation of the formation of coffee ring with spherical

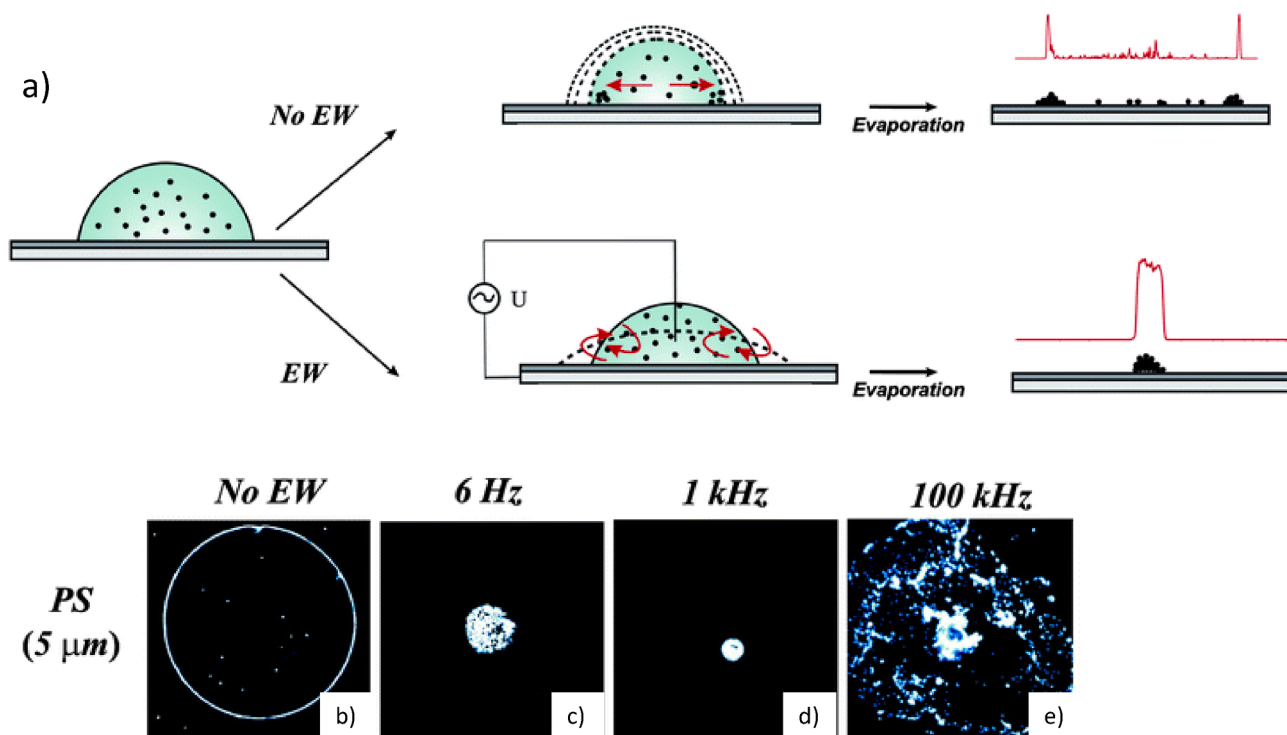


Fig. 6. a) Schematic representation of the drop evaporation process. Top row represents evaporation without electrowetting and with contact line pinning. Bottom row shows the process with electrowetting and mobile contact lines. b) – e) Suppression of coffee ring effect illustrated for PS particles at three frequency regimes (6 Hz, 1 kHz and 100 kHz). Reprint with permission from Royal Society of Chemistry 2011. Ref. [52].

solute particles (Fig. 7a), and ellipsoids (Fig. 7b). The spherical particles with $\alpha = 1.0$ formed a coffee ring pattern (Fig. 7a-right) whereas ellipsoids with $\alpha = 3.5$ formed a uniform deposition showing that the distortion from spherical shape suppressed the CRE (Fig. 7b-right). To confirm that this was due to interactions between the particle's surfactant was mixed with ellipsoids (Fig. 7c). This restored the CRE by hindering between the particle–particle interactions [56]. Similarly, V.R. Dugyala et al., demonstrated the suppression of CRE for submicron hematite ellipsoids. In this study, a uniform deposition was obtained by controlling the pH of the solution to overcome any residual repulsive forces between particles [57]. Thus, if the capillary forces are overcome by the strong particle interactions this can lead to a more uniform deposition [56,58,59].

3.4. Acoustics

The introduction of surface acoustic waves (SAWs) into the evaporating droplet can form both standing acoustic waves and standing capillary waves (Fig. 8). These waves generate standing wave patterns with nodes such that particles are trapped in the nodal regions of standing acoustic pressure waves with the distance between two adjacent nodal regions corresponding to one-half wavelength of the standing acoustic pressure waves (76 μm) as shown in Fig. 8. Thus, for example, Cooper et al. studied the suppression of the coffee ring effect by surface acoustic waves (SAWs) [60].

Polystyrene particles or silica particles of diameter ranging from 0.1 to 10 μm were dispersed in water and a droplet (2 μL) to evaporate when coupled with a SAWs of 9.7 MHz frequency and 1 W of power. After a few seconds, the majority of the particles were trapped in the nodal regions of capillary waves and accumulations of particles appeared at the liquid–gas interface [60]. This pressure gradient at the interface induced the local flow of the solute particles and trapped the particles on the substrate rather than moving toward the edge. The drag force exerted on the particles by the capillary flow was inferred to be less than the acoustic force, therefore no transport of the particles occurred. This

physical phenomenon is independent of the properties of the particles and the solvent [61,62].

3.5. Marangoni flow

The presence of a surface tension gradient over the liquid–air interface of the sessile droplet can result in a convective flow inside the droplet termed a Marangoni flow or stress. Either a small perturbation in the temperature [63] or solvents with different surface tension [64,65] may create a surface tension gradient, and thus a convective flow. In the former case, the thermal conductivities of the liquid and the substrate decide the direction of the Marangoni flow in any specific system. The ratio (k_r) of thermal conductivity of the substrate (k_s) and that of the liquid (k_l) was experimentally studied by Ristenpart et al., where $k_r = k_s/k_l$. In particular they investigated the flow of polystyrene particles (1 μm) in different volatile liquids on a polydimethylsiloxane substrate. Values of k_r less than 1.45 showed a radial inward flow of particles whereas when $k_r > 2$, then a radial outward flow was observed.

When an inward Marangoni flow is experienced in a droplet, its velocity is more than that of the outward capillary flow, which then forms a solute concentrated centre after evaporation. The Marangoni flow is less in the cases of aqueous solvents, especially pure water, but noticeable particularly in volatile non-aqueous liquids [65,66]. Larson and Hu observed Marangoni flow in octane, a volatile organic solvent [65]. A vortex in the drying octane droplet could be seen clearly (Fig. 9a). To observe the flow in the droplet, monodispersed 4.7 μm poly (methyl methacrylate) (PMMA) fluorescent particles were dispersed into octane as tracers to track Marangoni flow. Bright regions were produced by a combination of the lens effect and fluorescent PMMA particles. During the evaporation of the droplet, the temperature at the liquid–gas interface was not uniform due to the evaporative cooling. A simulation of the octane evaporation (Fig. 9b) showed that the temperature was the lowest and the surface tension was the highest at the liquid–gas interface caused by a longer thermal conduction path [65], which created an inward flow near the surface of the droplet. Larson also

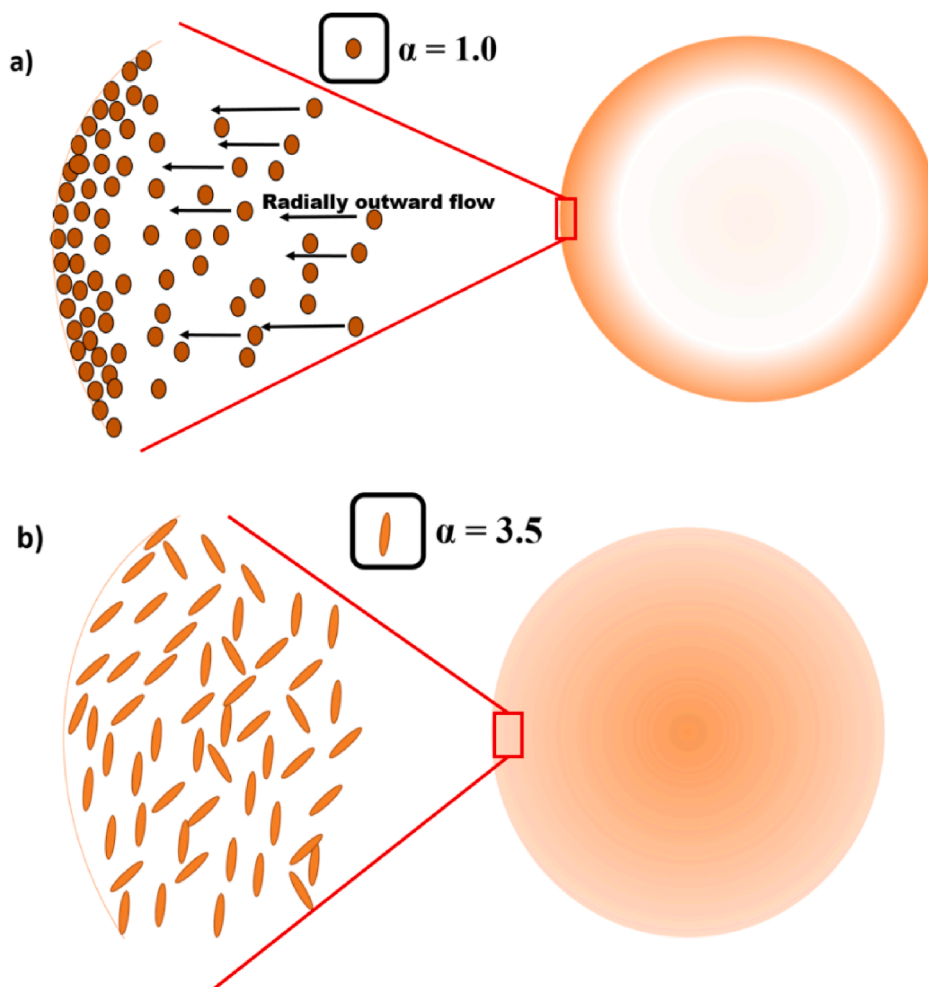


Fig. 7. Schematic representation of drying of spherical (a) and ellipsoidal (b) particles. Spheres are closely packed at the contact line with $\alpha = 1.0$ (a), Ellipsoids are uniformly distributed throughout the droplet due to interparticle attractions with $\alpha = 3.5$ (b).

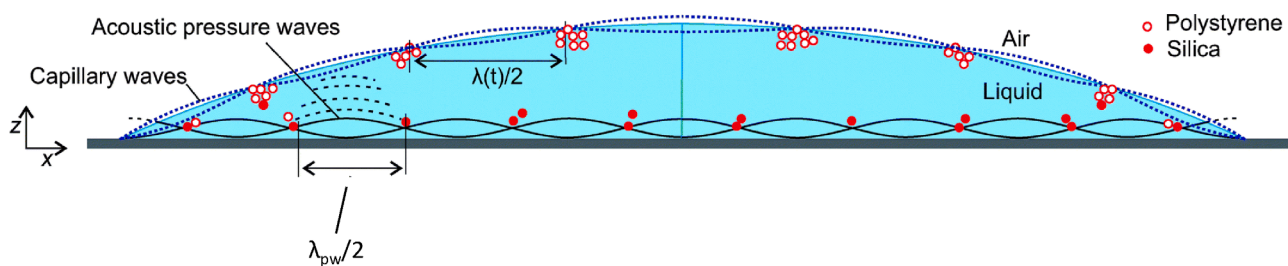


Fig. 8. Schematic illustration of a droplet excited by SAW. Abbreviation: λ_{pw} : wavelength of acoustic pressure waves, $\lambda(t)$: wavelength of capillary waves, SAW: surface acoustic waves. Reprinted with permission from Royal Society of Chemistry 2015. Ref. [60].

simulated the flow in a water droplet (Fig. 9c). They observed much weaker Marangoni flow in a water droplet without an inward flow compared with Fig. 9b. This explains why the coffee ring effect can often be observed more easily in an aqueous solution rather than in an organic solvent.

Marangoni flow can be enhanced by increasing the substrate temperature during the evaporation of a water droplet. Ta et al. applied laser irradiation to a polystyrene aqueous suspension [63] to create an inward flow in the water droplet (Fig. 9d). The laser beam locally heated up the droplet and the substrate, generated a temperature perturbation, then formed a Marangoni flow (yellow arrow in Fig. 9d) that counteracted the capillary flow (blue arrow in Fig. 9d), and thus reduced or suppressed the coffee ring effect. The time of application of the laser affected the

coffee ring effect. The formation of an optimally homogeneous distribution of PS particles required a specific amount of time from the laser beam (Fig. 9e). The main point of Marangoni flow is to create a temperature or pressure gradient so that an inward flow can be generated to reduce the capillary flow and the coffee ring effect. This is superior to other techniques in suppressing the coffee ring effect since it is independent of the system's chemical parameters [64,66–71].

4. Advice for electrochemists

Overall, all the five methods discussed above show a good ability to suppress the coffee ring effect. However, the creation of bespoke hydrophobic surfaces, and the use of electrowetting and acoustic methods

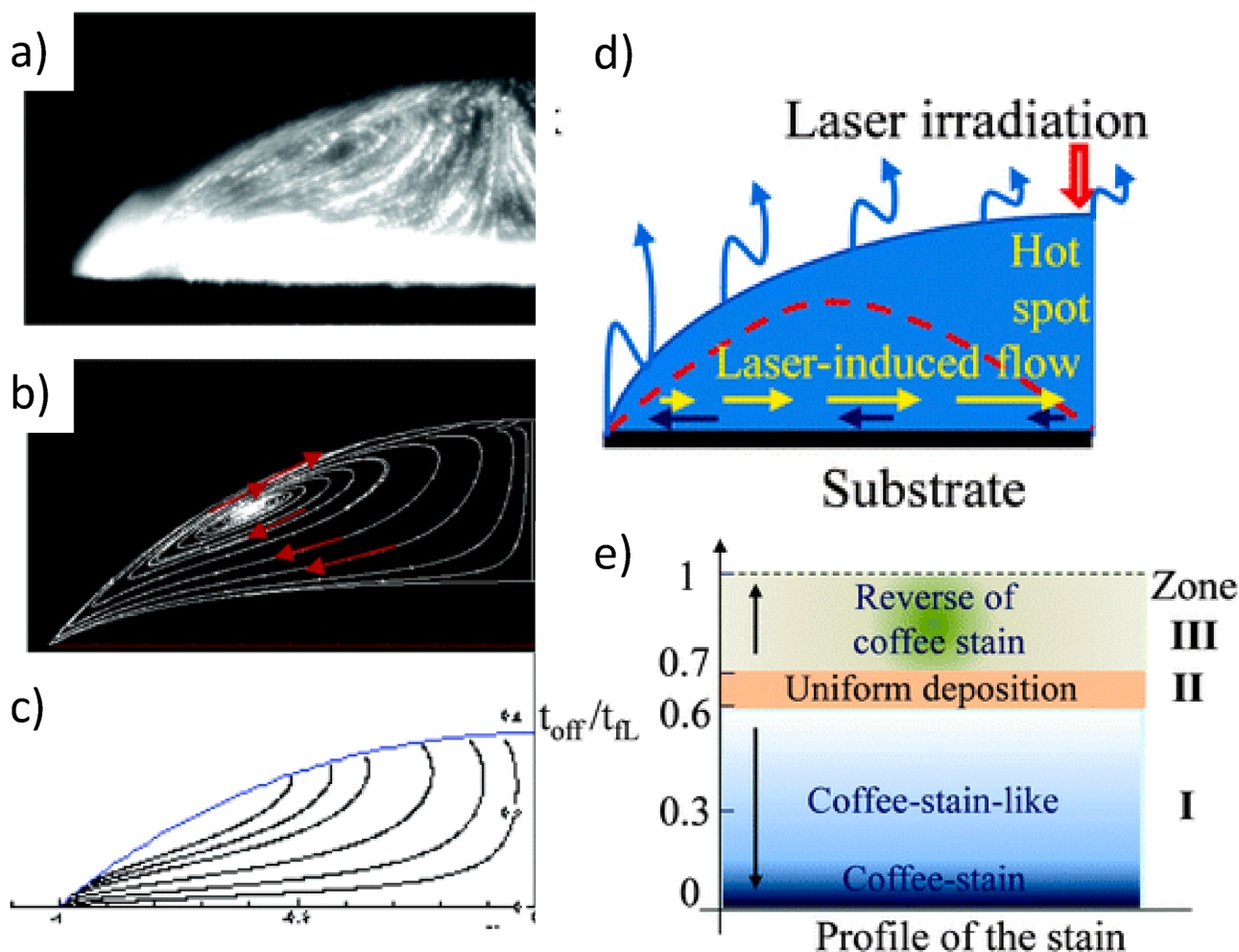


Fig. 9. Flow field in a drying octane droplet, a) imaged experimentally and b) predicted. c) simulated flow of a drying water droplet. Reprinted with permission from Hu and Larson. The Journal of Physical Chemistry B. 2006; 110(14):7090–4. Copyright (2006) American Chemical Society. Ref. [65]. d) Schematic diagram of the evaporation process of water droplet with laser irradiation at the centre. e) Characteristics of the formed patterns. Reprinted with permission from Royal Society of Chemistry 2016. Ref. [63].

are not realistic for most electrochemical purposes for self-evident reasons. Thus the most practical approach to adopt is to employ and explore in an empirical approach a variety of different solvents in combination with the microscopic imaging of surfaces to seek an optimal solvent in which Marangoni effects best mitigate coffee ring effects. At the same time it is important to recognise that organic solvents may also influence the reactivity under study and hence not play a purely passive role in the modification procedure [72,73].

5. Conclusions

Drop casting techniques are widely used in electrocatalytic analysis and electrochemical sensing techniques. The influence of the coffee ring effect can alter the distribution of the nano particles dropcasted on an electrode. Several strategies can be used to ameliorate this effect including using the Marangoni effect, anisotropic particles, or surfactants. These techniques can help in obtaining a uniform distribution of the drop casted nanoparticles across the area of the electrode.

CRediT authorship contribution statement

Archana Kaliyaraj Selva Kumar: Writing - original draft, Writing - review & editing. **Yifei Zhang:** Writing - original draft, Writing - review & editing. **Danlei Li:** Writing - review & editing. **Richard G. Compton:**

Conceptualization, Supervision, Resources.

Declaration of Competing Interest

The authors declare that they have no known competing financial interests or personal relationships that could have appeared to influence the work reported in this paper.

Acknowledgements

Archana K S thanks the Commonwealth Scholarship Commissions, UK for funding her DPhil research at the University of Oxford. D. Li thanks the China Scholarship Council and the University of Oxford for supporting her DPhil research.

References

- [1] K.E. Toghill, R.G. Compton, Electrochemical non-enzymatic glucose sensors: A perspective and an evaluation, *Int. J. Electrochem. Sci.* 5 (2010) 1246–1301.
- [2] J.H. Zagal, S. Griveau, J.F. Silva, T. Nyokong, F. Bedioui, Metallophthalocyanine-based molecular materials as catalysts for electrochemical reactions, *Coord. Chem. Rev.* 254 (2010) 2755–2791.
- [3] P. Si, Y.J. Huang, T.H. Wang, J.M. Ma, Nanomaterials for electrochemical non-enzymatic glucose biosensors, *RSC Adv.* 3 (2013) 3487–3502.
- [4] Z.L. Wang, Triboelectric nanogenerators as new energy technology for self-powered systems and as active mechanical and chemical sensors, *ACS Nano* 7 (2013) 9533–9557.

- [5] B.J. Sanghavi, O.S. Wolfbeis, T. Hirsch, N.S. Swami, Nanomaterial-based electrochemical sensing of neurological drugs and neurotransmitters, *Microchim. Acta* 182 (2015) 1–41.
- [6] M. Sajid, M.K. Nazal, M. Mansha, A. Alsharaa, S.M.S. Jillani, C. Basheer, Chemically modified electrodes for electrochemical detection of dopamine in the presence of uric acid and ascorbic acid: A review, *Trac-Trends Anal. Chem.* 76 (2016) 15–29.
- [7] P. Bollella, G. Fusco, C. Tortolini, G. Sanzo, G. Favero, L. Gorton, R. Antiochia, Beyond graphene: Electrochemical sensors and biosensors for biomarkers detection, *Biosens. Bioelectron.* 89 (2017) 152–166.
- [8] N. Baig, M. Sajid, T.A. Saleh, Recent trends in nanomaterial-modified electrodes for electroanalytical applications, *Trac-Trends Anal. Chem.* 111 (2019) 47–61.
- [9] A. Kamenev, A. Lyakhov, S. Orlov, Determination of arsenic (III) and copper (II) by stripping voltammetry in a mixed EDTA-phosphoric acid supporting electrolyte, *J. Anal. Chem.* 60 (2005) 156–162.
- [10] D. Kato, T. Kamata, D. Kato, H. Yanagisawa, O. Niwa, Au nanoparticle-embedded carbon films for electrochemical As³⁺ Detection with High Sensitivity and Stability, *Anal. Chem.* 88 (2016) 2944–2951.
- [11] M. Yang, X. Chen, J.H. Liu, X.J. Huang, Enhanced anti-interference on electrochemical detection of arsenite with nanoporous gold in mild condition, *Sens. Actuator B-Chem.* 234 (2016) 404–411.
- [12] J. Mafa, N. Mabuba, O. Arotiba, An exfoliated graphite based electrochemical sensor for As (III) in water, *Electroanalysis* 28 (2016) 1462–1469.
- [13] X. Dai, O. Nekrasova, M.E. Hyde, R.G. Compton, Anodic stripping voltammetry of arsenic (III) using gold nanoparticle-modified electrodes, *Anal. Chem.* 76 (2004) 5924–5929.
- [14] A.O. Simm, C.E. Banks, S.J. Wilkins, N.G. Karousos, J. Davis, R.G. Compton, A comparison of different types of gold-carbon composite electrode for detection of arsenic (III), *Anal. Bioanal. Chem.* 381 (2005) 979–985.
- [15] A. Salimi, M.E. Hyde, C.E. Banks, R.G. Compton, Boron doped diamond electrode modified with iridium oxide for amperometric detection of ultra trace amounts of arsenic (III), *Analyst* 129 (2004) 9–14.
- [16] E. Majid, S. Hrapovic, Y. Liu, K.B. Male, J.H. Luong, Electrochemical determination of arsenite using a gold nanoparticle modified glassy carbon electrode and flow analysis, *Anal. Chem.* 78 (2006) 762–769.
- [17] L. Rassaei, M. Sillanpää, R.W. French, R.G. Compton, F. Marken, Arsenite determination in phosphate media at electroaggregated gold nanoparticle deposits, *Electroanalysis (N.Y.N.Y.)* 20 (2008) 1286–1292.
- [18] C. Shen, S. Wang, Y. Jin, W.-Q. Han, In situ AFM imaging of solid electrolyte interfaces on HOPG with ethylene carbonate and fluoroethylene carbonate-based electrolytes, *ACS Appl. Mater. Interfaces* 7 (2015) 25441–25447.
- [19] O. Cherstniuk, P. Simonov, E. Savinova, Model approach to evaluate particle size effects in electrocatalysis: preparation and properties of Pt nanoparticles supported on GC and HOPG, *Electrochim. Acta* 48 (2003) 3851–3860.
- [20] Y. Wang, J.D. Zhang, Z.Y. Zhu, E.K. Wang, A carbon single crystal electrode for an electrochemical quartz crystal microbalance study, *J. Electroanal. Chem.* 419 (1996) 1–6.
- [21] S. Eloul, R.G. Compton, Voltammetric sensitivity enhancement by using preconcentration adjacent to the electrode: simulation, critical evaluation, and insights, *J. Phys. Chem. C* 118 (2014) 24520–24532.
- [22] L. Chen, E. Kätelhön, R.G. Compton, Unscrambling illusory inhibition and catalysis in nanoparticle electrochemistry: Experiment and theory, *Appl. Mater. Today* 16 (2019) 141–145.
- [23] E. Kätelhön, L. Chen, R.G. Compton, Nanoparticle electrocatalysis: Unscrambling illusory inhibition and catalysis, *Appl. Mater. Today* 15 (2019) 139–144.
- [24] E. Kätelhön, R.G. Compton, Unscrambling illusionary catalysis in three-dimensional particle-modified electrodes: Reversible reactions at conducting particles, *Appl. Mater. Today* 18 (2020), 100514.
- [25] L. Chen, E. Kätelhön, R.G. Compton, Particle-modified electrodes: General mass transport theory, experimental validation, and the role of electrostatics, *Appl. Mater. Today* 18 (2020), 100480.
- [26] E.E. Tanner, R.G. Compton, How can electrode surface modification benefit electroanalysis? *Electroanalysis* 30 (2018) 1336–1341.
- [27] T.J. Davies, R.R. Moore, C.E. Banks, R.G. Compton, The cyclic voltammetric response of electrochemically heterogeneous surfaces, *J. Electroanal. Chem.* 574 (2004) 123–152.
- [28] T.J. Davies, C.E. Banks, R.G. Compton, Voltammetry at spatially heterogeneous electrodes, *J. Solid State Electrochem.* 9 (2005) 797–808.
- [29] C.E. Banks, R.R. Moore, T.J. Davies, R.G. Compton, Investigation of modified basal plane pyrolytic graphite electrodes: definitive evidence for the electrocatalytic properties of the ends of carbon nanotubes, *ChemComm* (2004) 1804–1805.
- [30] T.J. Davies, M.E. Hyde, R.G. Compton, Nanotrench arrays reveal insight into graphite electrochemistry, *Angew. Chem., Int. Ed.* 44 (2005) 5121–5126.
- [31] C.E. Banks, T.J. Davies, G.G. Wildgoose, R.G. Compton, Electrocatalysis at graphite and carbon nanotube modified electrodes: edge-plane sites and tube ends are the reactive sites, *ChemComm* (2005) 829–841.
- [32] A. Einstein, On the motion of small particles suspended in liquids at rest required by the molecular-kinetic theory of heat, *Ann. Phys.* 17 (1905) 208.
- [33] H.S. Toh, R.G. Compton, ‘Nano-impacts’: An electrochemical technique for nanoparticle sizing in optically opaque solutions, *ChemistryOpen* 4 (2015) 261–263.
- [34] H. Toh, R. Compton, Electrochemical detection of single micelles through ‘nano-impacts’, *Chem. Sci.* 6 (2015) 5053–5058.
- [35] H.S. Toh, C. Batchelor-McAuley, K. Tschulik, C. Damm, R.G. Compton, A proof-of-concept—Using pre-created nucleation centres to improve the limit of detection in anodic stripping voltammetry, *Sens. Actuators, B* 193 (2014) 315–319.
- [36] H. Li, D. Buesen, R. Williams, J. Henig, S. Stapf, K. Mukherjee, E. Freier, W. Lubitz, M. Winkler, T. Happe, Preventing the coffee-ring effect and aggregate sedimentation by in situ gelation of monodisperse materials, *Chem. Sci.* 9 (2018) 7596–7605.
- [37] R.D. Deegan, O. Bakajin, T.F. Dupont, G. Huber, S.R. Nagel, T.A. Witten, Capillary flow as the cause of ring stains from dried liquid drops, *Nature* 389 (1997) 827–829.
- [38] H. Eral, J. Oh, Contact angle hysteresis: a review of fundamentals and applications, *Colloid Polym. Sci.* 291 (2013) 247–260.
- [39] J. Park, J. Moon, Control of colloidal particle deposit patterns within picoliter droplets ejected by ink-jet printing, *Langmuir* 22 (2006) 3506–3513.
- [40] M. Kuang, L. Wang, Y. Song, Controllable printing droplets for high-resolution patterns, *Adv. Mater.* 26 (2014) 6950–6958.
- [41] A. Friederich, J.R. Binder, W. Bauer, Rheological control of the coffee stain effect for inkjet printing of ceramics, *J. Am. Ceram. Soc.* 96 (2013) 2093–2099.
- [42] B.-J. de Gans, U.S. Schubert, Inkjet printing of well-defined polymer dots and arrays, *Langmuir* 20 (2004) 7789–7793.
- [43] J. Zou, F. Kim, Diffusion driven layer-by-layer assembly of graphene oxide nanosheets into porous three-dimensional macrostructures, *Nat. Commun.* 5 (2014) 1–9.
- [44] W. Han, Z. Lin, Learning from “Coffee Rings”: ordered structures enabled by controlled evaporative self-assembly, *Angew. Chem., Int. Ed.* 51 (2012) 1534–1546.
- [45] M. Anyfantakis, Z. Geng, M. Morel, S. Rudiuk, D. Baigl, Modulation of the coffee-ring effect in particle/surfactant mixtures: the importance of particle-interface interactions, *Langmuir* 31 (2015) 4113–4120.
- [46] Y.-F. Li, Y.-J. Sheng, H.-K. Tsao, Evaporation stains: suppressing the coffee-ring effect by contact angle hysteresis, *Langmuir* 29 (2013) 7802–7811.
- [47] H.-Y. Ko, J. Park, H. Shin, J. Moon, Rapid self-assembly of monodisperse colloidal spheres in an ink-jet printed droplet, *Chem. Mater.* 16 (2004) 4212–4215.
- [48] A.G. Marín, H. Gelderblom, A. Susarrey-Arce, A. van Houselt, L. Lefferts, J. G. Gardeniers, D. Lohse, J.H. Snoeijer, Building microscopic soccer balls with evaporating colloidal fakir drops, *Proc. Natl. Acad. Sci.* 109 (2012) 16455–16458.
- [49] L. Cui, J. Zhang, X. Zhang, Y. Li, Z. Wang, H. Gao, T. Wang, S. Zhu, H. Yu, B. Yang, Avoiding coffee ring structure based on hydrophobic silicon pillar arrays during single-drop evaporation, *Soft Matter* 8 (2012) 10448–10456.
- [50] D. Tian, Y. Song, L. Jiang, Patterning of controllable surface wettability for printing techniques, *Chem. Soc. Rev.* 42 (2013) 5184–5209.
- [51] M. Dicuango, S. Dash, J.A. Weibel, S.V. Garimella, Effect of superhydrophobic surface morphology on evaporative deposition patterns, *Appl. Phys. Lett.* 104 (2014), 201604.
- [52] H.B. Eral, D.M. Augustine, M.H. Duits, F. Mugele, Suppressing the coffee stain effect: how to control colloidal self-assembly in evaporating drops using electrowetting, *Soft Matter* 7 (2011) 4954–4958.
- [53] F. Li, F. Mugele, How to make sticky surfaces slippery: Contact angle hysteresis in electrowetting with alternating voltage, *Appl. Phys. Lett.* 92 (2008), 244108.
- [54] F. Mugele, J.-C. Baret, Electrowetting: from basics to applications, *J. Phys.: Condens. Matter* 17 (2005) R705.
- [55] T.A. Nguyen, M.A. Hampton, A.V. Nguyen, Evaporation of nanoparticle droplets on smooth hydrophobic surfaces: the inner coffee ring deposits, *J. Phys. Chem. C* 117 (2013) 4707–4716.
- [56] P.J. Yunker, T. Still, M.A. Lohr, A.G. Yodh, Suppression of the coffee-ring effect by shape-dependent capillary interactions, *Nature* 476 (2011) 308–311.
- [57] V.R. Dugyala, M.G. Basavaraj, Control over coffee-ring formation in evaporating liquid drops containing ellipsoids, *Langmuir* 30 (2014) 8680–8686.
- [58] D. Stamou, C. Duschl, D. Johannsmann, Long-range attraction between colloidal spheres at the air-water interface: The consequence of an irregular meniscus, *Phys. Rev. E* 62 (2000) 5263.
- [59] S. Dasgupta, M. Katava, M. Faraj, T. Auth, G. Gompper, Capillary Assembly of Microscale ellipsoidal, cuboidal, and spherical Particles at Interfaces, *Langmuir* 30 (2014) 11873–11882.
- [60] D. Mampallil, J. Reboud, R. Wilson, D. Wylie, D.R. Klug, J.M. Cooper, Acoustic suppression of the coffee-ring effect, *Soft Matter* 11 (2015) 7207–7213.
- [61] S. Mhatre, A. Zigelman, L. Abezgauz, O. Manor, Influence of a propagating megahertz surface acoustic wave on the pattern deposition of solute mass off an evaporating solution, *Langmuir* 32 (2016) 9611–9618.
- [62] X. Ding, P. Li, S.-C.-S. Lin, Z.S. Stratton, N. Nama, F. Guo, D. Slotcavage, X. Mao, J. Shi, F. Costanzo, Surface acoustic wave microfluidics, *Lab Chip* 13 (2013) 3626–3649.
- [63] V. Ta, R. Carter, E. Esenturk, C. Connaughton, T.J. Wasley, J. Li, R.W. Kay, J. Stringer, P. Smith, J.D. Shephard, Dynamically controlled deposition of colloidal nanoparticle suspension in evaporating drops using laser radiation, *Soft Matter* 12 (2016) 4530–4536.
- [64] H. Jin, J. Qian, L. Zhou, J. Yuan, H. Huang, Y. Wang, W.M. Tang, H.L.W. Chan, Suppressing the coffee-ring effect in semitransparent MnO₂ film for a high-performance solar-powered energy storage window, *ACS Appl. Mater. Interfaces* 8 (2016) 9088–9096.
- [65] H. Hu, R.G. Larson, Marangoni effect reverses coffee-ring depositions, *J. Phys. Chem. B* 110 (2006) 7090–7094.
- [66] R.D. Deegan, Pattern formation in drying drops, *Phys. Rev. E* 61 (2000) 475.
- [67] W. Ristenpart, P. Kim, C. Domingues, J. Wan, H.A. Stone, Influence of substrate conductivity on circulation reversal in evaporating drops, *Phys. Rev. Lett.* 99 (2007), 234502.
- [68] P. Li, Y. Li, Z.K. Zhou, S. Tang, X.F. Yu, S. Xiao, Z. Wu, Q. Xiao, Y. Zhao, H. Wang, Evaporative self-assembly of gold nanorods into macroscopic 3D plasmonic superlattice arrays, *Adv. Mater.* 28 (2016) 2511–2517.

- [69] E. Talbot, A. Berson, C. Bain, Drying and deposition of picolitre droplets of colloidal suspensions in binary solvent mixtures, in: NIP & Digital Fabrication Conference, Society for Imaging Science and Technology, 2012, pp. 420–423.
- [70] H. Hu, R.G. Larson, Analysis of the effects of Marangoni stresses on the microflow in an evaporating sessile droplet, *Langmuir* 21 (2005) 3972–3980.
- [71] V.X. Nguyen, K.J. Stebe, Patterning of small particles by a surfactant-enhanced Marangoni-Bénard instability, *Phys. Rev. Lett.* 88 (2002), 164501.
- [72] E.I. Rogers, N.S. Lawrence, R.G. Compton, The electrochemical oxidation of ruthenocene in various room temperature ionic liquids, *J. Electroanal. Chem.* 657 (2011) 144–149.
- [73] C. Batchelor-McAuley, L.M. Gonçalves, L. Xiong, A.A. Barros, R.G. Compton, Controlling voltammetric responses by electrode modification; using adsorbed acetone to switch graphite surfaces between adsorptive and diffusive modes, *ChemComm* 46 (2010) 9037–9039.